"Bending to Stretching" Transition in Disordered Networks

Gavin A. Buxton and Nigel Clarke
Department of Chemistry, University of Durham, Durham, DH1 3LE, United Kingdom
(Received 31 January 2007; published 7 June 2007)

From polymer gels to cytoskeletal structures, random networks of elastic material are commonly found in both materials science and biology. We present a three-dimensional micromechanical model of these networks and identify a "bending-to-stretching" transition. We characterize this transition in terms of concentration scaling laws, the stored elastic energy, and affinity measurements. Understanding the relationship between microscopic geometry and macroscopic mechanics will elucidate, for example, the mechanical properties of polymer gel networks or the role of semiflexible network mechanics in cells.

DOI: 10.1103/PhysRevLett.98.238103 PACS numbers: 87.16.Ka, 62.20.Dc

Common structural features link cellular materials [1,2], polymer gels [3,4], and biological networks [5–7]: that of a random lattice of interconnecting struts. These struts can bear mechanical loads by either stretching or bending. Interestingly, some materials appear to macroscopically deform primarily through the local stretching of the struts, while in other materials the elastic energy is stored via local bending. Furthermore, a transition between these two regimes has been reported. Wilhelm and Frey (2003) and Head *et al.* (2003) simulated the two-dimensional elastic deformation of a network of rods [8–10]. A transition from a system where the macroscopic elasticity was dominated by the bending stiffness of the struts, to where the stretching stiffness dominated, was observed with increasing rod density. Head *et al.* (2003) characterized this transition as being from a system with a nonuniform strain field (nonaffine) to a system with a uniform strain field (affine) [9,10]. Onck *et al.* (2005) have also observed such a transition for systems under very large deformations, where the struts align in the tensile direction [11]. Furthermore, experimental studies have also observed this transition and, in particular, Liu *et al.* have directly imaged the strain field in semiflexible polymer networks and observed less affinely deformed networks in the bending regime [12]. Elucidating this transition is not only of interest to materials scientists but is also vital to our understanding of various biological systems, from cellular structures, such as wood and trabecular bone [1], to actin and cytoskeletal networks [5]. The purpose of the Letter, therefore, is to present our computational study of the elasticity of randomly generated three-dimensional lattice structures and to quantify the geometry dependence of the bending-to-stretching transition. Whereas previous studies have investigated this transition in terms of the density of overlapping rods in two-dimensional systems, here we characterize this transition as a function of three-dimensional lattice connectivity. In particular, we present the elastic moduli as a function of the concentration of struts and describe the affinity of these deformations, in order to facilitate comparisons with experimental studies.

We use a bond-bending lattice spring model (LSM) to capture the deformation of random networks of interconnected struts. In particular, the LSM consists of lattice sites connected by one-dimensional harmonic interactions. The LSM is traditionally considered to consist of a regular lattice and is adopted from condensed matter theory [13] and molecular simulations [14]. The regular LSM has been shown to capture linear elasticity theory [15,16] and simulate material heterogeneity [16–24]. Furthermore, Ladd *et al.* [25,26] have used a regular LSM to capture the deformation of trabecular bone. In contrast, in the present work we assume that each strut can be captured using a simple harmonic interaction and define the compressive or stretching and bending force constants as $k_{\|} = E_s A/l$ and $k_{\perp} = 12E_s I/l^3$, respectively. The force constants depend on E_s, the material Young's modulus, A, the cross-sectional area (πr^2), I, the area moment of inertia of the struts ($\pi r^4/4$), and l, the length of the strut. We take E_s to be unity and the radius of the rods, r, to be 0.1 in dimensionless units. This allows us to capture the micromechanics of large systems.

The elastic energy of a Born LSM can be written in matrix form as [16] $A_i = \frac{1}{2}\sum_{ij}\mathbf{u}_{ij}\cdot\mathbf{M}_{ij}\cdot\mathbf{u}_{ij}$, where A_i is the elastic energy stored at node i, the summation is over neighboring nodes, $\mathbf{u}_{ij}$ is the difference in nodal displacements (i.e., $\mathbf{u}_i - \mathbf{u}_j$), and $\mathbf{M}_{ij}$ is a matrix of elastic constants. For a strut in the [100] direction the force constants can be chosen to mimic the tensile and bending rigidity of a cylindrical strut, resulting in a matrix of the form

$$\mathbf{M}_{[100]} = \begin{pmatrix} k_{\|} & 0 & 0 \\ 0 & k_{\perp} & 0 \\ 0 & 0 & k_{\perp} \end{pmatrix}. \quad (1)$$

We can use this matrix to obtain the matrix of force constants for struts of any orientation through appropriate rotational transformations [16]. By minimizing the energy of this linear system of equations and balancing the forces at nodal points, we can equilibrate an irregular lattice of such struts and obtain macroscopic elastic constants.

We construct our three-dimensional networks by first randomly distributing LSM nodes throughout the system. We then connect neighboring nodes by struts. In particular, nodes within a given distance are connected and this distance is chosen in order to maintain an average connectivity in the lattice. Struts which would be connected in the x direction, in the presence of periodic boundary conditions, are redefined as boundary struts and used to connect the LSM lattice with the system boundaries. Free boundary conditions are applied in the y and z directions. It should be noted that the system described here focuses only on mechanical deformations while it has been reported that thermal fluctuations can also play a role in semiflexible polymer networks [27]. The effects of these thermal fluctuations are believed to increase the effective compliance of the struts as the applied deformation has to first pull out thermal fluctuations before stretching the polymer backbone.

A rigid percolation transition has been observed in disordered networks. For very low densities the struts have been found to be isolated, or in small clusters, and macroscopically the network does not percolate [9]; a similar rigidity percolation has been found by Hough *et al.* [28] in carbon nanotube suspensions. In our simulations we find that for systems with an average connectivity of three or less the material does not resist small deformations. As we increase the connectivity, however, the lattice forms a percolating pathway of rigid material and the material is macroscopically capable of bearing applied loads.

Figure 1 shows two lattices of different connectivity and under different deformations. Figures 1(a) and 1(c) depict systems with a low density of nodes, but high connectivity (on average 15) and Figs. 1(b) and 1(d) depict systems with a high density of nodes, but low connectivity (on average 5); the concentration of struts, however, is roughly 0.06 in all systems. Despite the similarity in concentration, the geometry of the systems are clearly different. Arrows indicate the direction of applied deformation (either shear or normal). The system boundaries (whose displacement drives the deformation) are depicted as gray walls, and the struts are colored from white (relatively undeformed) to red (high stretching energy) or blue (high bending energy). It can, therefore, be seen that the systems with higher and lower connectivity deform primarily through the stretching and bending of the lattice struts, respectively.

Bending dominated deformation throughout the system has previously been associated with nonaffine strain fields [9,10] and a lower density of struts [8,10]. The bending regime occurs because the system can deform without the struts having to change length. Rather, the distances between lattice nodes remain relatively unchanged and the angles between struts varies. The bending rigidity of the lattice struts is proportional to the area moment of inertia ($\propto R^4$, where R is the radius of the struts), while the concentration is proportional to the cross-sectional area ($\propto R^2$). From scaling arguments, therefore, the macroscopic rigidity (either Young's or shear modulus) should scale as concentration squared [1].

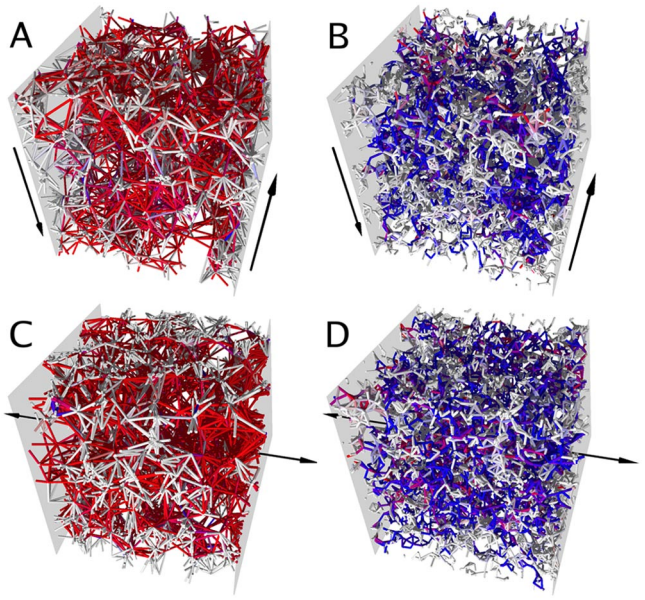

FIG. 1 (color online). Deformed networks subject to shear (a), (b) and normal (c), (d) deformations (arrows indicate direction of applied deformation). Both high connectivity (a), (c) and low connectivity (b), (d) systems are shown. Struts are colored white if relatively undeformed, blue if the deformation energy of the struts is predominantly bending, and red if the deformation energy is predominantly stretching.

In contrast to the bending regime, the stretching occurs because the system cannot deform without changing the length of the struts. In particular, such rigidity is thought to arise from clusters of triangles [29] or, more precisely, a network composed of many triangular tessellations. In such structures, a change in the position of a lattice node necessarily causes changes to the lengths of the neighboring struts. As the stretching rigidity of the lattice struts is proportional to the cross-sectional area, the macroscopic rigidity should scale linearly with concentration (which is also proportional to cross-sectional area). From the scaling arguments of Gibson [1] a change in the exponent (in the elastic modulus versus concentration plots) from 2 to 1 indicates a change from bending-to-stretching dominated deformation.

Figure 2 shows both the relative shear modulus and relative Young's modulus as a function of concentration. For each value of connectivity we consider five different values for the number of lattice nodes ($N = 500$, 1000, 2000, 4000, 8000). Furthermore, we equilibrate three independent geometries for each connectivity and lattice node specification. The mechanical properties of these randomly generated geometries are displayed in Fig. 2. Increasing the connectivity of the geometry increases the number of struts and, therefore, the concentration, shear modulus, and Young's modulus all increase. Furthermore, the gradients of the log-log plots of shear and Young's

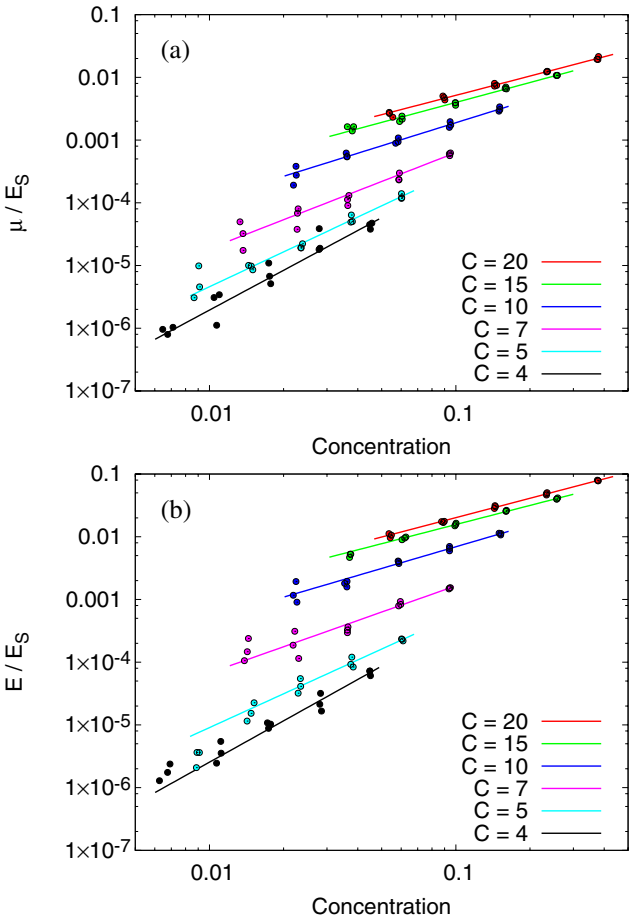

FIG. 2 (color online). Graph to show (a) relative shear modulus and (b) relative Young's modulus as a function of concentrations. Systems with lattice connectivities of 4, 5, 7, 10, 15, and 20 are compared. Points represent simulation data and solid lines are fitted curves.

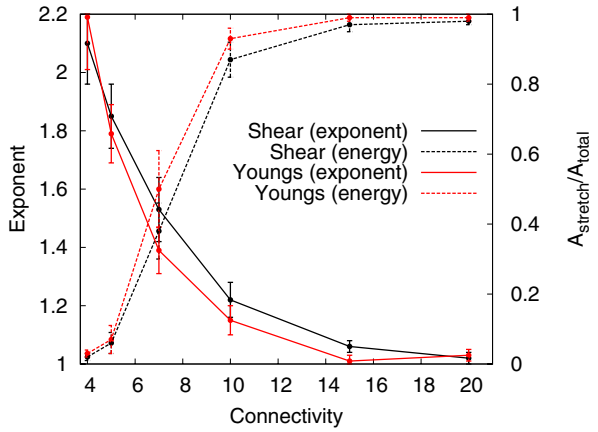

FIG. 3 (color online). Graph to show both concentration scaling law exponent (left axis) and the ratio of stretching to total elastic energy (right axis) as a function of lattice connectivity. Bending-to-stretching transition is observed in systems subject to both shear and tensile deformations at a connectivity of ~7.

modulus versus concentration appear to decrease with increasing connectivity. Recall that this is expected from scaling arguments as systems with high connectivity should deform primarily through stretching.

We quantify this transition in Fig. 3. We characterize the bending-to-stretching transition using the exponent obtained from Fig. 2 and the ratio of stretching energy to total energy. The exponent varies from ~2 at low connectivity to ~1 at high connectivity, in agreement with predictions based entirely on scaling arguments. On the second y axis of Fig. 3 we depict the ratio of elastic energy due entirely to the stretching of the struts with the total elastic energy. The ratio between stretching and total energy does not depend on the concentration, but on the microscopic connectivity of the network. We, therefore, average this quantity over all the struts, in all systems with a given connectivity. This ratio is ~0 for low connectivity which indicates that most of the elastic energy is stored through bending deformations. For higher connectivities the ratio approaches 1 indicating that the elastic energy in the deformed system arises from the stretching of the struts.

Finally, we measure the affinity of the deformation fields in these disordered systems. In Fig. 4(a) we plot the relative displacement ($u_x/L\epsilon$, where u_x is displacement, L is system length, and ϵ is applied strain) as a function of initial position for two systems under normal deformation. The solid line depicts a perfectly affine deformation; the high ($C = 20$) and low ($C = 4$) connectivity systems are represented by circles and stars, respectively. While systems of low and high connectivity show disorder, the system with low connectivity exhibits collections of points which possess similar displacements for large ranges of initial position [horizontal lines of star points in Fig. 4(a)]. This is due to clusters which do not contribute to the percolating structure (and do not, therefore, support stress) but exist in a relatively undeformed state attached to the percolating structure. Furthermore, the inset of Fig. 4(a) shows the degree of nonaffinity, defined as $R(\Delta r_0) = \langle((\Delta r_{ij} - \Delta r_{ij}^A)/\Delta r_{ij}^A)^2\rangle$, where Δr_{ij} is the distance between nodes i and j, Δr_{ij}^A is the affine distance, and Δr_0 is the unperturbed distance. Consistent with earlier work [10,12] the degree of nonaffinity decreases with distance (the deformations appear more uniform over larger distances). The connectivity appears to affect the affinity of the deformation field equally, for all length scales.

To quantify the nonaffine nature of the deformations we plot the root-mean-square (rms) deviation of simulated positions from those of perfectly affine deformations. Furthermore, we plot a standard correlation function between the displaced and initial positions (for a perfectly affine deformation this equals 1). Figure 4(b) shows both the decrease in this rms deviation (solid line) and the increase in the correlation function (dashed line) for systems with increasing connectivity. Therefore, consistent with previous studies, we find the bending-to-stretching transition to be accompanied by a change towards more uniform deformation fields.

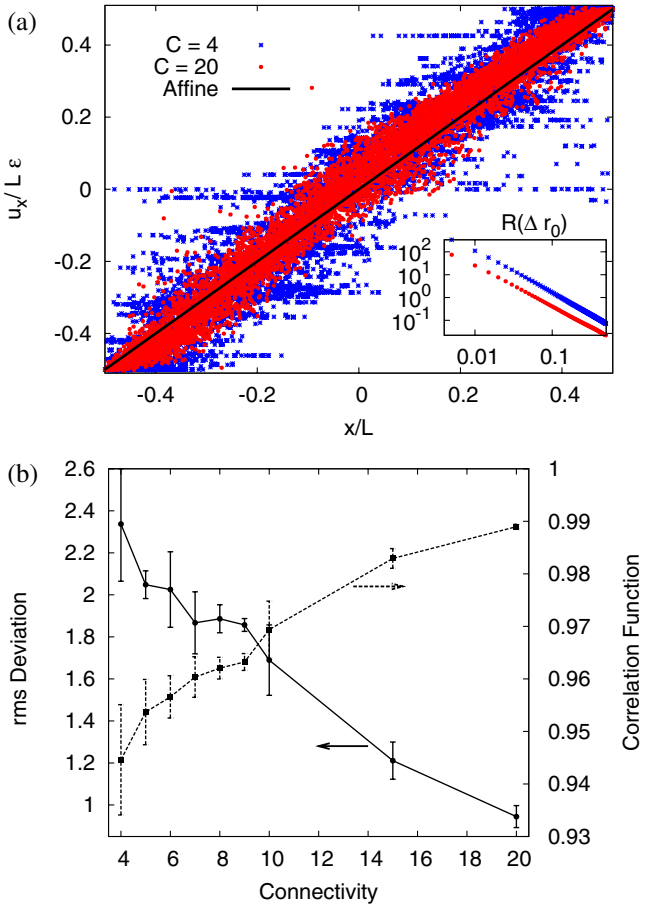

FIG. 4 (color online). (a) Relative displacement vs distance for systems of high ($C = 20$) and low ($C = 4$) connectivity (degree of nonaffinity depicted in inset). (b) rms deviation of displacements from perfectly affine deformation, and correlation function between displacement and distance, as a function of connectivity.

To summarize, the bending-to-stretching transition is found to be a continuous geometry-dependent transition in the three-dimensional lattice networks considered here. In particular, the transition occurs as a function of the average connectivity of the disordered elastic network. We quantify this transition in terms of the concentration scaling laws, the stored elastic energy, and affinity measurements. Understanding this bending-to-stretching transition is important for predicting structure-property relations in materials such as cellular structures and polymer gels and elucidating the role of mechanics in biological networks.

[1] L. J. Gibson and M. F. Ashby, Proc. R. Soc. A **382**, 43 (1982).
[2] L. J. Gibson, J. Biomech. **38**, 377 (2005).
[3] L. Applegarth, N. Clarke, A. C. Richardson, A. D. M. Parker, I. Radosavljevic-Evans, A. E. Goeta, J. A. K. Howard, and J. W. Steed, Chem. Commun. (Cambridge) 43 (2005) 5423.
[4] C. E. Stanley, N. Clarke, K. M. Anderson, J. A. Elder, J. T. Lenthall, and J. W. Steed, Chem. Commun. (Cambridge) 30 (2006) 3199.
[5] M. J. Gardel, J. H. Shin, F. C. MacKintosh, L. Mahadevan, P. Matsudaira, and D. A. Weitz, Science **304**, 1301 (2004).
[6] A. R. Bausch and K. Kroy, Nature Phys. **2**, 231 (2006).
[7] B. A. DiDonna and A. J. Levine, Phys. Rev. Lett. **97**, 068104 (2006).
[8] J. Wilhelm and E. Frey, Phys. Rev. Lett. **91**, 108103 (2003).
[9] D. A. Head, A. J. Levine, and F. C. MacKintosh, Phys. Rev. E **68**, 061907 (2003).
[10] D. A. Head, A. J. Levine, and F. C. MacKintosh, Phys. Rev. Lett. **91**, 108102 (2003).
[11] P. R. Onck, T. Koeman, T. van Dillen, and E. van der Giessen, Phys. Rev. Lett. **95**, 178102 (2005).
[12] J. Liu, G. H. Koenderink, K. E. Kasza, F. C. MacKintosh, and D. A. Weitz, arXiv:cond-mat/0702323v1.
[13] M. Born and K. Huang, *Dynamical Theory of Crystal Lattices* (Clarendon, Oxford, 1954).
[14] W. T. Ashurst and W. G. Hoover, Phys. Rev. B **14**, 1465 (1976).
[15] L. Monette and M. P. Anderson, Model. Simul. Mater. Sci. Eng. **2**, 53 (1994).
[16] G. A. Buxton, C. M. Care, and D. J. Cleaver, Model. Simul. Mater. Sci. Eng. **9**, 485 (2001).
[17] L. Monette, M. P. Anderson, S. Ling, and G. S. Grest, J. Mater. Sci. **27**, 4393 (1992).
[18] M. Ostoja-Starzewski, P. Y. Sheng, and I. Jasiuk, J. Eng. Mater. Technol. **116**, 384 (1994).
[19] L. Monette, M. P. Anderson, and G. S. Grest, J. Appl. Phys. **75**, 1155 (1994).
[20] G. A. Buxton and A. C. Balazs, J. Chem. Phys. **117**, 7649 (2002).
[21] G. A. Buxton and A. C. Balazs, Phys. Rev. E **67**, 031802 (2003).
[22] G. A. Buxton and A. C. Balazs, Phys. Rev. B **69**, 054101 (2004).
[23] A. C. Balazs and G. A. Buxton, in *Encyclopedia of Nanoscience and Nanotechnology* (Marcel Dekker, New York, 2004), p. 3785.
[24] G. A. Buxton and A. C. Balazs, Macromolecules **38**, 488 (2005).
[25] A. J. C. Ladd, J. H. Kinney, and T. M. Breunig, Phys. Rev. E **55**, 3271 (1997).
[26] A. J. C. Ladd and J. H. Kinney, Physica (Amsterdam) **240A**, 349 (1997).
[27] F. C. MacKintosh, J. Käs, and P. A. Janmey, Phys. Rev. Lett. **75**, 4425 (1995).
[28] L. A. Hough, M. F. Islam, P. A. Janmey, and A. G. Yodh, Phys. Rev. Lett. **93**, 168102 (2004).
[29] M. Kellomaki, J. Astrom, and J. Timonen, Phys. Rev. Lett. **77**, 2730 (1996).